Structural Defects and the Origin of the Second Length Scale in $SrTiO_3$

Renhui Wang* and Yimei Zhu
Department of Applied Science, Brookhaven National Laboratory, Upton, New York 11973

S. M. Shapiro
Department of Physics, Brookhaven National Laboratory, Upton, New York 11973
(Received 24 July 1997)

To understand the origin of the second long-length scale in $SrTiO_3$, we studied structural defects in Verneuil-grown single crystals by transmission electron microscopy. The density of the dislocations was observed to decrease with increasing depth from the original cut surface of the crystals. The high density of dislocations in the skin region is most likely responsible for the second length scale. [S0031-9007(98)05447-7]

PACS numbers: 64.70.Kb, 77.80.Bh, 77.84.Dy

The cubic-to-tetragonal phase transition at a temperature $T_c \sim 100$ K in perovskite $SrTiO_3$ is driven by the softening of a zone-boundary R point $(\frac{1}{2}\frac{1}{2}\frac{1}{2})$ phonon mode [1]. According to the theory of critical phenomena, there should be a single correlation length $\xi = 2\pi/\kappa$, where the inverse correlation length κ is proportional to the half width at half maximum of a diffraction peak profile across the R point, which is broad and Lorentzian. Inelastic neutron studies [1] showed that the Lorentzian profile is due to the soft mode with dispersion $\omega^2(q, T) = \omega(0, T) + \alpha q^2$, where the momentum q is measured relative to the R point and $\omega^2(0, T) \sim (T - T_c)$. In addition to the phonon sidebands, subsequent neutron studies [2] reported an elastic peak that has come to be called the central peak, whose intensity diverges as T_c is approached. About ten years ago, Andrews [3], using high resolution x-ray diffraction, observed an unexpected, narrow Lorentzian-squared peak in addition to the usual broad one. This finding implies the existence of a second long-length scale ξ_{L2} and the corresponding inverse correlation length κ_{L2}. From systematic studies of the two length scales [4–7], it was concluded that the narrow component was dominant in the "skin" region of the sample where the strain concentration was higher, and might be induced by a higher concentration of defects near the surface. Nevertheless, there has been no direct observation of the defects and their distribution in the skin region of the $SrTiO_3$ crystals, nor have the defects giving rise to the central peak been identified. In this Letter, we report our study of structural defects and their distribution in Verneuil-grown $SrTiO_3$ single crystals by transmission electron microscopy (TEM) to find the origin of the second length scale and the central peak near the cubic-to-tetragonal phase transition.

The very same single-crystal slices of 0.5 mm thickness, which showed the two-length-scale phenomena by x-ray and neutron experiments (referred to as AC-0.5 in Ref. [7], supplied by Atomergic Chemicals Co., and grown by the Verneuil method), were carefully cut into small pieces for our *in situ* TEM study. To compare the TEM observations with the x-ray and neutron diffraction results, the cross-section samples were prepared without modifying the original surface. For each sample, two crystal slices, with their original surfaces against each other, were sandwich glued by two Si slabs. The sample was then sliced perpendicularly to the surfaces and ion milled at low temperature using Gatan low-energy guns at very shallow angles ($<10°$).

Figures 1(a) and 1(b) are typical TEM images showing the morphology of structural defects in the AC-0.5 sample using reflections $\mathbf{g} = (-200)$ and $\mathbf{g} = (020)$, respectively. B is denoted as bubble, and D as dislocation. A systematic contrast experiment and defocus convergent-

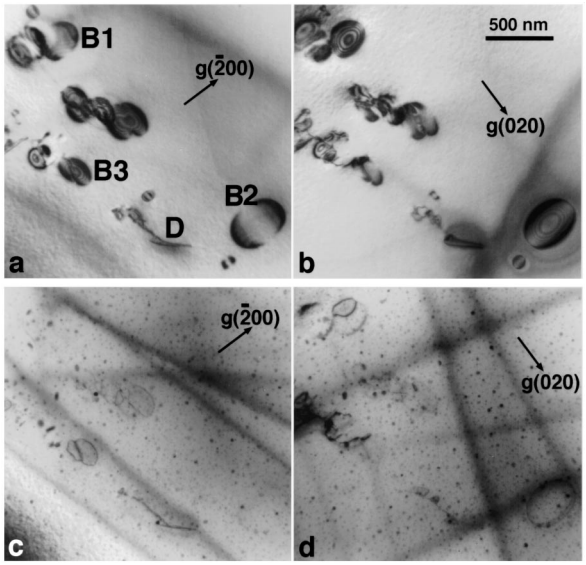

FIG. 1. Bright-field images showing structural defects and the annealing effects in the $SrTiO_3$ crystal using reflections $\mathbf{g} = (-200)$ [(a) and (c)] and $\mathbf{g} = (020)$ [(b) and (d)]. B is denoted as bubble, and D as dislocation. (a), (b) before heating, (c), (d) heated at 650 K for 30 min and then cooled to RT. Note the dot contrast from nanoscale bubbles and dislocation loops in (c) and (d).

 0031-9007/98/80(11)/2370(4)$15.00

beam electron diffraction analysis revealed that most dislocations have a Burgers vector of $\mathbf{b} = a\langle 110\rangle$. The dislocations are usually of mixed character with both screw and edge components. The bubbles range from about 10 to 500 nm in diameter, featured by annular thickness fringes at their interface with the crystal matrix, and a line of no contrast perpendicular to the imaging reciprocal vectors resulting from a radial strain field surrounding them, as shown in Figs. 1(a) and 1(b). When irradiated by a focused incident beam or heated above 625 K using an *in situ* heating stage, the bubbles, especially those in thin areas of the crystal, shrink, collapse, and eventually disappear. Figures 1(c) and 1(d) are taken from the same area as Fig. 1(a) after the sample had been heated in the microscope for 30 min at 650 K and then cooled to room temperature. In addition to the loops left by shrunken bubbles after heating, much smaller defects (about 15–50 nm in diameter) formed [seen as dot contrast in Figs. 1(c) and 1(d)]; they are nanoscale bubbles and dislocation loops with a $\langle 100\rangle$ Burgers vector. During irradiation by the focused incident electron beam, we observed small dislocation loops hopping from one position to another. From these experiments, and the process of crystal growth described by Bednorz and Scheel [8], we conclude that supersaturated gases were absorbed by the $SrTiO_3$ single crystals during their flame-fusion growth and then precipitated as gas bubbles during cooling. These nanoscale bubbles and associated dislocation loops appear throughout the sample.

Study of the variation of defect density with depth away from the original cut surface in cross-section samples revealed a very steep dislocation distribution in the skin region of the AC-0.5 crystals. However, there was no gradient in distribution of bubbles. The dislocation density at the original cut surface is very high, see Fig. 2(a), and decreases with depth as shown in Fig. 2(b). Figure 3 plots the dislocation density as a function of depth from the cut surface of the crystals. The density is about $6 \times 10^9/\mathrm{cm}^2$ at the cut surface, decreases very steeply to $1 \times 10^9/\mathrm{cm}^2$ at about 10 μm, and then declines to a constant level $(1 \sim 2) \times 10^8/\mathrm{cm}^2$ at about 20 μm. This observation suggests that a higher dislocation concentration near the cut surface, inducing a heterogeneous strain distribution, may give rise to a quasistatic narrow length component.

Our TEM experiments were mainly *in situ* using either a heating stage or a cooling stage, although the dislocation density was measured at room temperature. During cooling, we directly observed the symmetry change of the crystal lattice near the dislocation core using convergent beam electron diffraction (CBED), suggesting a phase transition initiated at the defects. Quantitative analysis of the phase transition was not possible because of the unknown temperature due to the heating of the focused electron beam, and to the blurry lines in the CBED pattern due to the strain field associated with the defects. Our

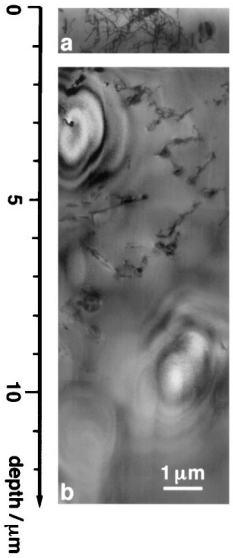

FIG. 2. Dislocation distribution (a) at the cut surface and (b) near the surface in the cross-section AC-0.5 sample showing a marked depth dependence of dislocation density.

in situ experiments, however, inspired us to pursue an analysis of strain-induced nucleation centers for the phase transition.

A rough estimate of the mean stress caused by these dislocations was obtained using a similar approach as that by Altarelli *et al.* [9]. The elastic constants for $SrTiO_3$ at room temperature are $C_{11} = 316$ GPa, $C_{12} = 102$, and $C_{44} = 123$ GPa (at $80 \sim 300$ K, the elastic constants vary by less than 8% [10,11]) with an anisotropy ratio $A = 2C_{44}/(C_{11} - C_{12}) = 1.15$, which suggests that the crystal is nearly isotropic. Based on the linear elasticity theory for isotropic solids [12], the trace of the stress tensor at a point (r, ϕ) from an edge dislocation is

$$\sigma = -\frac{\mu b(1 + p)}{\pi(1 - p)} \frac{\sin\phi}{r}, \tag{1}$$

where $\mu = C_{44} = (C_{11} - C_{12})/2$ is the shear modulus, b is the Burgers vector length, $p = C_{12}/(C_{11} + C_{12})$

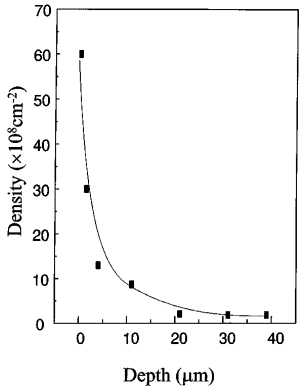

FIG. 3. Dislocation density as a function of the depth from the cut surface.

Poisson's ratio, and ϕ is the angle from the x axis which is parallel to the Burgers vector $\mathbf{b}$. The mean square of the stress σ over the region from b to R may be calculated from Eq. (1):

$$\langle \sigma^2 \rangle = \left(\frac{\mu b(1 + p)}{\pi(1 - p)} \right)^2 \frac{1}{R^2} \ln \frac{R}{b} . \quad (2)$$

Substituting experimental values for μ, p, and b into Eq. (2), we found that, in an area close to an edge dislocation, the stress is quite large, e.g., $\sigma = 9.1$ GPa when $R/b = 10$. Equations (1) and (2) indicate that there is an approximate power-law decay for the stress field of a dislocation $\sigma(r) \sim r^{-a}$ with $a \sim 1$; for bubbles, $a = 3$.

Based on Landau's theory, we assume that the free energy of the tetragonal $SrTiO_3$ is lowered in the strained regions when the spontaneous strains of the tetragonal domains are close to the existing strains in the specimen. We can express quantitatively the lowering of the free energy by using the Landau free-energy density:

$$F = \tfrac{1}{2} a[T - (T_c + K\sigma)]Q^2 + \tfrac{1}{4} BQ^4 + \cdots , \quad (3)$$

where Q is the order parameter in the Landau's theory which is the rotation angle of the octahedra in the tetragonal $SrTiO_3$, σ is the stress, and K and B are constants. The term $-\frac{1}{2} aK\sigma Q^2$ is the lowest nonvanishing coupling term between the stress and the order parameter. Equation (3) indicates an increase of the transition temperature from T_c to $(T_c + K\sigma)$ caused by the existence of the stress σ. At a given temperature T ($>T_c$), those regions can be transformed into a low-temperature phase, where the stress is larger than that determined by the condition

$$T - T_c - K\sigma = 0 . \quad (4)$$

Okai and Yoshimoto [11] determined experimentally the pressure dependence of the transition temperature in $SrTiO_3$ and found a mean value for $K = dT_c/d\sigma$ to be equal to 28 K/GPa when the pressure is increased from 0 to 3 GPa. Such a value was also calculated theoretically [13]. Taking this value, we estimated that the increase of the transition temperature in a region close to an edge dislocation (from $R/b = 1$ to $R/b = 10$) is about 255 K. This is not surprising since Osterman, Mohanty, and Axe [14] reported a surface transition temperature of $T_s = 340$ K, compared to the bulk transition temperature of $T_b = 112$ K for a polished, unetched Verneuil-grown $SrTiO_3$ crystal.

From Eq. (2), we know the relationship between the length R and the mean stress over the region from b to R around an edge dislocation. Using the relationship between stress and transition temperature experimentally measured by Okai and Yoshimoto [11], we obtained the length scale R of the stressed region, which has transformed into the low-temperature tetragonal phase at a given temperature T, around a dislocation line. The values $\kappa = 2\pi/R$ as a function of T (marked by open circles in Fig. 4) are in good coincidence with

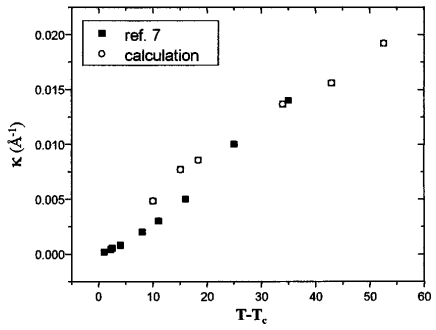

FIG. 4. Temperature dependence of the inverse correlation length $\kappa_{L2} = 2\pi/\xi_{L2}$ for the long-length scale measured by Hirota *et al.* [7] (solid squares) and calculated by the present model (open circles) using ξ_{L2} equal to the length scale R of the stressed region around a dislocation.

the temperature dependence of the inverse correlation length κ_{L2} for the narrow component measured by Hirota *et al.* [7] (marked by solid squares). Thus, we conclude that the so-called second length scale ξ_{L2} corresponds to the length scale R of the stressed regions which have transformed to the low-temperature phase at a temperature $T > T_c$ in the vicinity of dislocation lines.

Our observations are consistent with almost all of the experimental results [15,16]:

(i) Usually, mechanical processing causes an increase in dislocation density so that the narrow component induced by high density dislocations is observed for most crystals studied. Chemical etching can remove the surface layer, high-temperature annealing may reduce the dislocation density, and, hence, reduce its contribution to the narrow component [3,17].

(ii) Although the domain shape of the low-temperature phase is anisotropic with respect to the line direction, the dislocations themselves are neither straight nor parallel, and sometimes form tangles, as shown in Fig. 2(a). This fact is consistent with the observations [4,7] that the narrow component is almost isotropic.

(iii) Since the narrow component has a different origin than the broad component, the critical exponent ν_{L2} for the second correlation length ξ_{L2} defined by $\xi_{L2} \sim t^{-\nu_{L2}}$ [$t = (T - T_c)/T_c$], or $\kappa_{L2} \sim t^{\nu_{L2}}$ with $\xi_{L2} = 2\pi/\kappa_{L2}$, and the susceptibility exponent γ_{L2} defined as $\chi_{L2} \sim t^{-\gamma_{L2}}$, where χ_{L2} is the amplitude of the narrow component, must differ from those of the broad component. The components ν_{L2} and γ_{L2} may be estimated as follows.

From Eqs. (1) and (2), we have $\sigma = \sigma_0 R^{-1}$. Substituting into Eq. (4), we obtain the length of the domains of the low-temperature phase as

$$R = (K\sigma_0)^{-1}(T - T_c)^{-1} \sim t^{-1}, \quad (5)$$

which leads to $\nu_{L2} = 1$ if we take the domain length R of the low-temperature phase as the long-length scale ξ_{L2}. The integrated intensity I_{L2} of the narrow component is proportional to the quantity of the low-temperature phase,

and, hence, to R^2. By substituting Eq. (5), we obtain

$$I_{L2} \sim t^{-2}. \quad (6)$$

For a Lorentzian-squared profile $I_{L2} \sim \chi_{L2}\kappa_{L2}$, so that a rough estimate for the susceptibility exponent can be obtained,

$$\chi_{L2} \sim I_{L2}\xi_{L2} \sim t^{-3}, \quad (7)$$

which gives $\gamma_{L2} \sim 3$.

The critical exponent ν_{L2} was measured as 0.50 over the reduced temperature range $0.002 < t < 0.03$ [4], and about 1.27 over the range $0.01 < t < 0.35$ deduced from Hirota's data [7]. Our estimation of $\nu_{L2} = 1$ lies in between these values. The experimental value of $\gamma_{L2} = 2.6$ was deduced [15] from the data of McMorrow *et al.* [4] which approaches the estimated value of 3. The temperature dependence of the integrated intensity of the narrow component ($I_{L2} \sim t^{-2}$) estimated in Eq. (6) is also consistent with the experiments. Andrews [3] reported a constant linewidth ($\kappa_{L2} \sim t^0$) by low resolution measurement, and a t^{-2} temperature dependence for the amplitude χ_{L2}. These lead to $I_{L2} \sim \chi_{L2}\kappa_{L2} \sim t^{-2}$. From McMorrow *et al.* [4], we also have $I_{L2} \sim \chi_{L2}\kappa_{L2} \sim t^{-2.1}$. Moreover, the data given by Hirota *et al.* [7] for specimen AC-0.5 show $I_{L2} \sim t^{-1.8}$.

(iv) Our observation revealed that the surface layer with high dislocation density is nearly 1–3 μm thick. This result is consistent with the depth dependence of the narrow component experimentally studied by Hirota *et al.* [7], who found no depth dependence for penetration depths of 0.19–2.70 μm. Our result is also consistent with the depth dependence of the x-ray intensity of superreflection (311)/2 measured by Darlington and O'Connor [17], who found no depth dependence in the penetration range of 1.9–2.7 μm but evident dependence when the penetration depth increased from 2.7 to 5.0 μm, and to 8.1 μm. Recent diffraction measurements [18] show that the strain is much larger in the surface region of $\sim$10 μm than it is in the bulk.

(v) According to our model, the narrow component of the scattering above T_c originates from the low-temperature phase, so it should be centered at the position of the Bragg reflection of the low-temperature phase. This is difficult to verify for a $SrTiO_3$ crystal because of its low tetragonality ($c/a \sim 1.0005$). However, Ryan *et al.* [19] observed such a phenomenon in $RbCaF_3$.

(vi) The distribution of defects of both dislocations and bubbles in our AC-0.5 crystals is uneven, and, in some regions distant from the corners and edges of the sample, we did not observe as steep a distribution as shown in Fig. 3. This is consistent with residual stress measurements in damaged $SrTiO_3$ single crystals [20], where the highest residual stress exists near the corners. The unevenness of the defect distribution will affect the relative intensity of the narrow component in different regions of the specimen.

(vii) The bubbles and small dislocation loops are not localized near the surface and appear throughout the samples studied. These may be the defects giving rise to the central peak observed in all neutron studies of $SrTiO_3$. The central peak might arise from a local distortion of the lattice around such a defect, similar to the origin of Huang diffuse scattering observed near Bragg peaks. Our observations show that the bubbles annealed out at a temperature about 600 K; this suggests a neutron-diffraction experiment in which the sample is heated to 600 K and the central peak measured again to ascertain any change in intensity. An early optical study [21] in potassium dihydrogen phosphate showed the central peak is suppressed by annealing.

This research was supported by the U.S. Department of Energy, Division of Materials Science, Office of Basic Energy Sciences under Contract No. DE-AC02-76CH00016.

*On leave from Department of Physics, Wuhan University, Wuhan 430072, People's Republic of China.

[1] G. Shirane and Y. Yamada, Phys. Rev. **177**, 858 (1969).
[2] S. M. Shapiro, J. D. Axe, G. Shirane, and T. Riste, Phys. Rev. B **6**, 4332 (1972).
[3] S. R. Andrews, J. Phys. C **19**, 3721 (1986).
[4] D. F. McMorrow, N. Hamaya, S. Shimomura, Y. Fujii, S. Kishimoto, and H. Iwasaki, Solid State Commun. **76**, 443 (1990).
[5] G. Shirane, R. A. Cowley, M. Matsuda, and S. M. Shapiro, Phys. Rev. B **48**, 15 595 (1993).
[6] H.-B. Neumann, U. Rutt, J. R. Schneider, and G. Shirane, Phys. Rev. B **52**, 3981 (1995).
[7] K. Hirota, J. P. Hill, S. M. Shapiro, G. Shirane, and Y. Fujii, Phys. Rev. B **52**, 13 195 (1995).
[8] J. G. Bednorz and H. J. Scheel, J. Cryst. Growth **41**, 5 (1977).
[9] M. Altarelli, M. D. Nunez-Regueiro, and M. Papoular, Phys. Rev. Lett. **74**, 3840 (1995).
[10] R. O. Bell and G. Rupperecht, Phys. Rev. **129**, 90 (1963).
[11] B. Okai and J. Yoshimoto, J. Phys. Soc. Jpn. **39**, 162 (1975).
[12] J. P. Hirth and J. Lothe, *Theory of Dislocations* (McGraw-Hill, New York, 1968).
[13] W. Zhong and D. Vanderbilt, Phys. Rev. Lett. **74**, 2587 (1995).
[14] D. P. Osterman, K. Mohanty, and J. D. Axe, J. Phys. C **21**, 2635 (1988).
[15] R. A. Cowley, Phys. Scr. **T66**, 24 (1996).
[16] R. A. Cowley, Philos. Trans. R. Soc. London A **354**, 2799 (1996).
[17] C. N. W. Darlington and D. A. O'Connor, J. Phys. C. **9**, 3561 (1976).
[18] U. Rütt, A. Diederichs, J. Strempfer, J. R. Schneider, and G. Shirane (to be published).
[19] T. W. Ryan, R. J. Nelmes, R. A. Cowley, and A. Gibaud, Phys. Rev. Lett. **56**, 2704 (1986).
[20] K. Aso, Jpn. J. Appl. Phys. **15**, 1243 (1976).
[21] E. Courtens, Phys. Rev. Lett. **41**, 1171 (1978).